

*promoting access to White Rose research papers*



**Universities of Leeds, Sheffield and York**  
**<http://eprints.whiterose.ac.uk/>**

---

This is an author produced version of a paper published in **Indoor and Built Environment**.

White Rose Research Online URL for this paper:  
<http://eprints.whiterose.ac.uk/7785/>

---

**Published paper**

Fletcher, L.A., Noakes, C.J., Sleight, P.A., Beggs, C.B. and Shepherd, S.J. (2008) *Air ion behavior in ventilated rooms*. *Indoor and Built Environment*, 17 (2). pp. 173-182.

<http://dx.doi.org/10.1177/1420326X08089622>

---

## **Air ion behaviour in ventilated rooms**

L.A. Fletcher<sup>1</sup>, C.J. Noakes<sup>1</sup>, P.A. Sleight<sup>1</sup>, C.B. Beggs<sup>2</sup>, S.J. Shepherd<sup>2</sup>

<sup>1</sup> Pathogen Control Engineering Research Group, School of Civil Engineering, University of Leeds, Leeds, LS2 9JT, UK

<sup>2</sup> School of Engineering, Design and Technology, University of Bradford, Bradford, BD7 1DP, UK

Corresponding author: Dr Catherine J Noakes, Email: [C.J.Noakes@leeds.ac.uk](mailto:C.J.Noakes@leeds.ac.uk),  
Tel: +44(0)113 343 2306

**Keywords:** negative, air ioniser, ventilation, electrical deposition, indoor air

## Abstract

Air ionisers have seen increasing use as devices for improving indoor air quality, including applications designed to reduce the transmission of infection in healthcare environments. However, little attention has been given to understanding and quantifying the physical behaviour of ions in indoor air. This study presents experimental data and a theoretical model to examine the factors that influence the concentration of ions in a ventilated room. The results demonstrate how, with an ioniser in operation, the ion concentration is governed by ion-ion interactions and electrical deposition at the walls, with the ventilation rate having a minimal influence. The results also demonstrate that an ion concentration greater than  $10^{10}$  ions/m<sup>3</sup> is necessary for these electrical effects to be significant, which has implications for the suitability of an ioniser for a particular location.

## 1. Introduction

In recent years there has been renewed interest in the use of air ionisers to improve indoor air quality, including reducing the transmission of infection in hospitals [1]. This has led many device manufacturers to produce air ionisers for use in domestic and commercial settings, which claim to remove dust, allergens and bioaerosols from room air. Such devices generally blow a stream of positive or negative air ions into room air, where they remove particulate matter through increased gravitational deposition and electrostatic attraction to walls and other surfaces [2]. Several authors have also presented evidence that air ions may have a biocidal effect [3-5] and may be effective as part of infection control strategies against some airborne pathogens [1].

The term 'air ion' is a generic term used to describe charged molecules or clusters of molecules in the air. Most ionisers utilize a corona discharge method to generate air ions. This is an electrical discharge brought on by the ionisation of the air surrounding an electrode when the potential gradient exceeds a critical value, with the result that a plasma is created around the electrode. Positive and negative coronas both involve an electron avalanche in the ionisation process. Such avalanches occur when strong electric fields act on free electrons in the air. The electric field accelerates the electrons so that they gain sufficient kinetic energy to cause ionisation when they collide with neutral gas molecules in their path. However, although often lumped together in the general category 'air ions', negative and positive air ions are profoundly different from each other. In a positive corona discharge the electron avalanche accelerates towards the electrode, with the result that fully formed primary positive ions are repelled into the atmosphere. By contrast, in a negative corona the electrons are generated at the electrode by the photoelectric action of photons striking its surface. These electrons are then repelled from the negative electrode into the atmosphere where they combine with neutral gas molecules to form primary negative ions, which have a structure based around  $O_2^-$  [6]. Further negative ions are then produced including the hydrate  $O_2^-(H_2O)_n$ , and secondary chemical species  $CO_4^-(H_2O)_n$ ,  $NO^-(H_2O)_n$  and  $NO_2^-(H_2O)_n$  [3]. The principle positive ion found in air is the hydronium ion  $H^+(H_2O)_n$  [6,7]. Once created, primary ions rapidly grow in size as they collide, first with neutral molecules in the air, and then with aerosol particles [8].

While much is known about corona discharge and the propagation of ions in air, relatively little is known about the practical application of ionisers in the indoor environment. The lack of data quantifying the physical behaviour of ions in ventilated rooms means that designers and engineers currently have little firm evidence on which to make important decisions regarding their application. Although experimental studies have demonstrated that negative ionisers have the potential to significantly reduce the concentration of particulates in indoor

air [2,9,10], theoretical models to complement these studies are very limited. Analytical models describing generic ion behaviour and the ion balance in outdoor air have been presented by a number of authors [6,11,12]. These have characterized the mobility of air ions and their rate of combination with ions of opposite polarity and particles in the external environment. However with regard to the indoor environment, the only notable work modelling ioniser behaviour is an analytical study of Mayya et al [2], which presented a detailed mathematical formulation describing the behaviour of negative ions and particles under time dependant conditions.

This paper presents both an experimental study and a theoretical model for characterizing the behaviour of air ions in ventilated room spaces. The study considers the influence of several factors including the ventilation rate, particle concentration, ion-ion interaction and wall deposition on the concentration of positive and negative ions in indoor air.

## 2. Experimental Methods

The experimental work described below was undertaken in a 32m<sup>3</sup> (4.25 x 3.35 x 2.5m high) climatically controlled, ventilated aerosol test chamber at the University of Leeds, which was maintained at a small negative pressure (approximately -10 Pa). This chamber has a HEPA filtered ventilation system, which allowed the air flow rate to be varied between 0.0089 and 0.133 m<sup>3</sup>/s (approximately 1 - 15 air changes per hour (AC/h)). The geometry of the chamber and the location of the devices and instrumentation within it, were as shown in Figure 1. During experimentation air entered the chamber at low level at a constant rate through diffuser I and was extracted at high level through diffuser II.

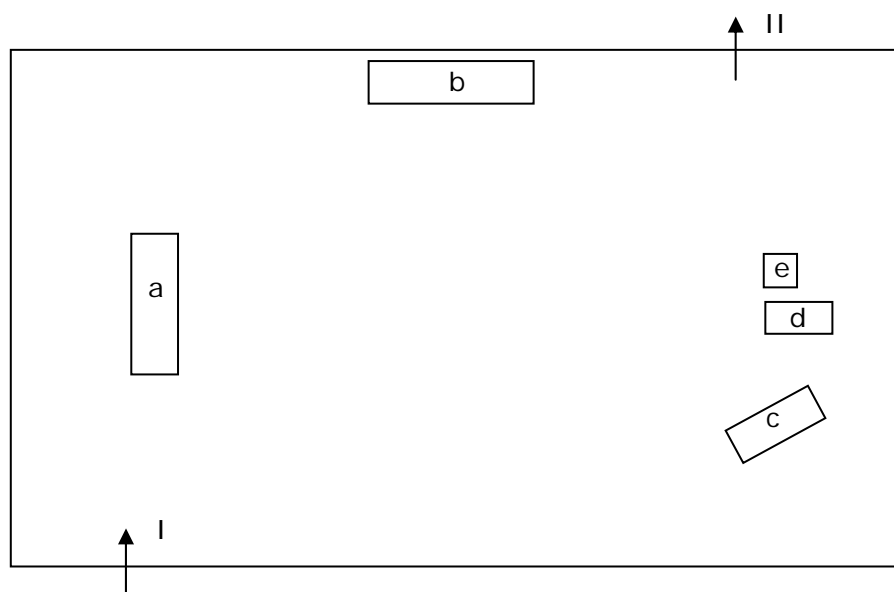


Figure 1: Plan view of test chamber and location of ionisers and instrumentation.  
(a: Plasmacluster ioniser, b: Aircare ioniser, c: Medion ion counter, d: Inti logging ion counter, e: laser particle counter, I: air inlet, II: air outlet)

Two ionisers were used in the study, a WM 120 Aircare ioniser (Air Ion Technologies Limited, New Milton, UK) which generated only negative ions, and a Plasmacluster device (Sharp, UK) which generated either negative ions only, or when operated in 'bipolar mode' generated both positive and negative ions. Both devices contained particulate filters and fans which recirculated room air through the ioniser unit. During the experiments the

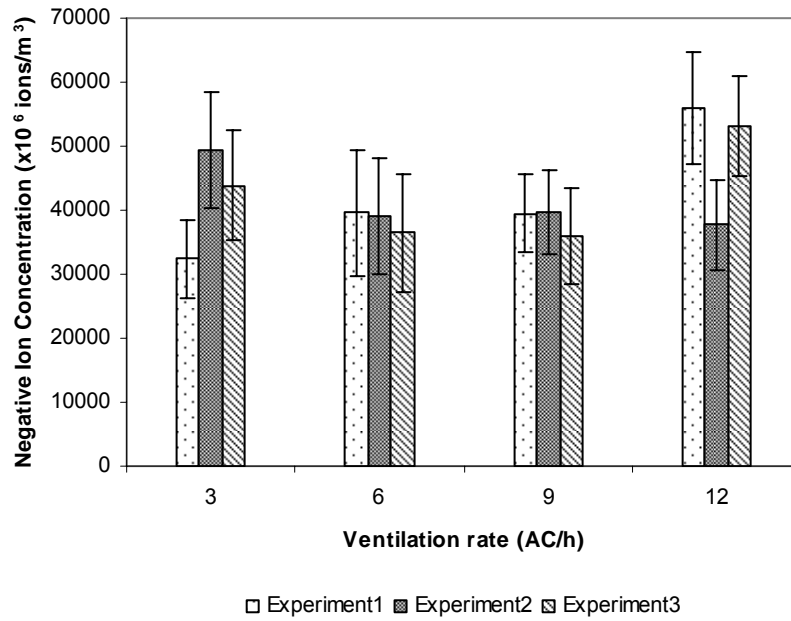
Plasmacluster ioniser was located at position (a) and the Aircare ioniser located at position (b), as shown in Figure 1.

The ion concentrations in the chamber were measured using either a logging ion counter (Inti ITC-201A, Andes Electrical Corporation, Japan), which recorded the ion concentration every 0.5s, or a Medion (Air Ion Technologies, Hants, UK) air ion analyser which required readings to be recorded manually. These counters were located on the opposite side of the chamber to the ionisers, at locations (c) and (d) in Figure 1. In addition, the concentration of airborne particles in the chamber was recorded throughout the experiments using a Kanomax Geo- $\alpha$  laser particle counter (Optical Sciences, UK). This recorded mean particle concentrations for particle diameters of 0.3-0.5, 0.5-1, 1-3, 3-5 and  $>5\mu\text{m}$  in the chamber at intervals of 5 minutes. Because of technical limitations it was not possible to record the concentration of particles  $< 0.3\mu\text{m}$  in diameter.

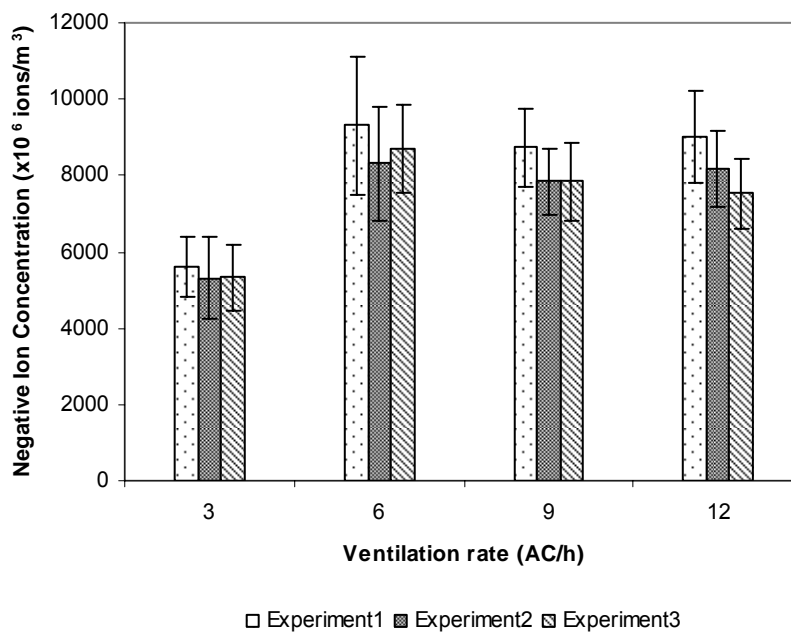
During the study two experimental regimes were utilized; firstly experiments were carried out to measure the ion concentration under steady-state conditions, and then a series of decay experiments were undertaken to assess the effect of the ventilation rate on the ion concentration when the ionisers were switched off. The steady-state experiments were carried out with an ioniser generating continuously over a period of 120 minutes. The ventilation rate was initially set at 3 AC/h and was then increased to 6, 9 then 12 AC/h at 30 min intervals. During this period the ion and particle concentrations were logged continually. In total, nine steady-state experiments were carried out; three using the Aircare negative ioniser, three using the Plasmacluster ioniser generating negative ions only, and three using the Plasmacluster device in bipolar mode, with only the positive ion concentration monitored. The decay experiments were also carried out for ventilation rates in the range 3-12 AC/h. However, for these experiments the ioniser was only in operation for 30 minutes, in order to achieve a steady-state ion concentration, before being switched off. With the ventilation system still in operation the decay in the ion concentration in the room was recorded every minute for the first five minutes and then every 5 minutes over the next 25 minutes using the Medion analyser. For each of the ionisers, four decay test runs were undertaken (i.e. at 3, 6, 9 and 12 AC/h respectively).

### **3. Experimental Results**

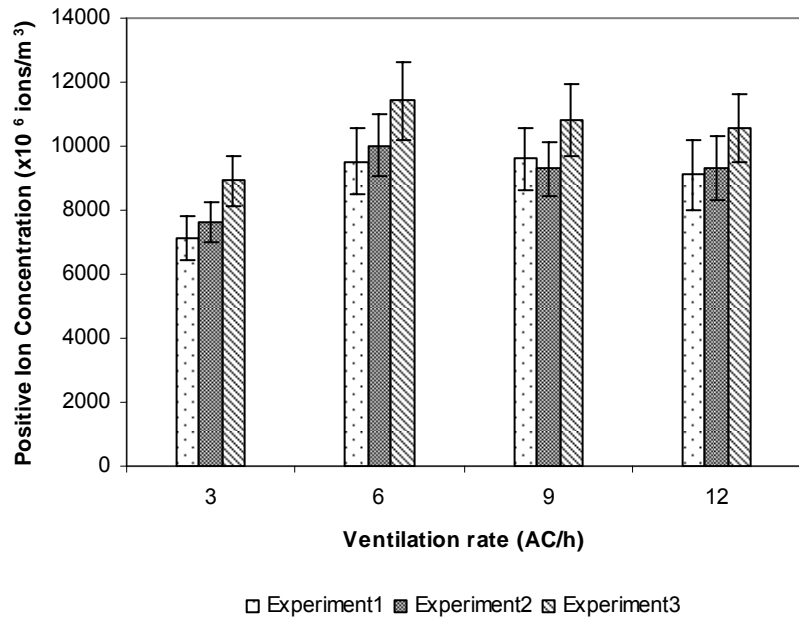
The results of the steady-state experiments are presented in Figure 2. These show the mean ion concentrations at the four ventilation rates for the Aircare ioniser, the Plasmacluster ioniser generating negative ions only, and the Plasmacluster device in bipolar mode, with only the positive ion concentration monitored. In each case results are presented from three replicate experiments where the ion concentration was logged for 30 minutes at each ventilation rate. However as the ion concentration during first 20 minutes at each ventilation rate may be transient, means and standard deviations were calculated using only the data collected in the final 10 minutes at each ventilation rate; a time period when the conditions could be reasonably assumed to be steady-state. From these figures a clear consistent picture emerges, namely, that the ventilation rate has little effect on the ion concentration (be it positive or negative) in the chamber. This behaviour was consistent for both ionisers, despite the fact that the Aircare ioniser produces considerably more ions than the Plasmacluster device.



(a) Negative ion concentrations for Aircare device

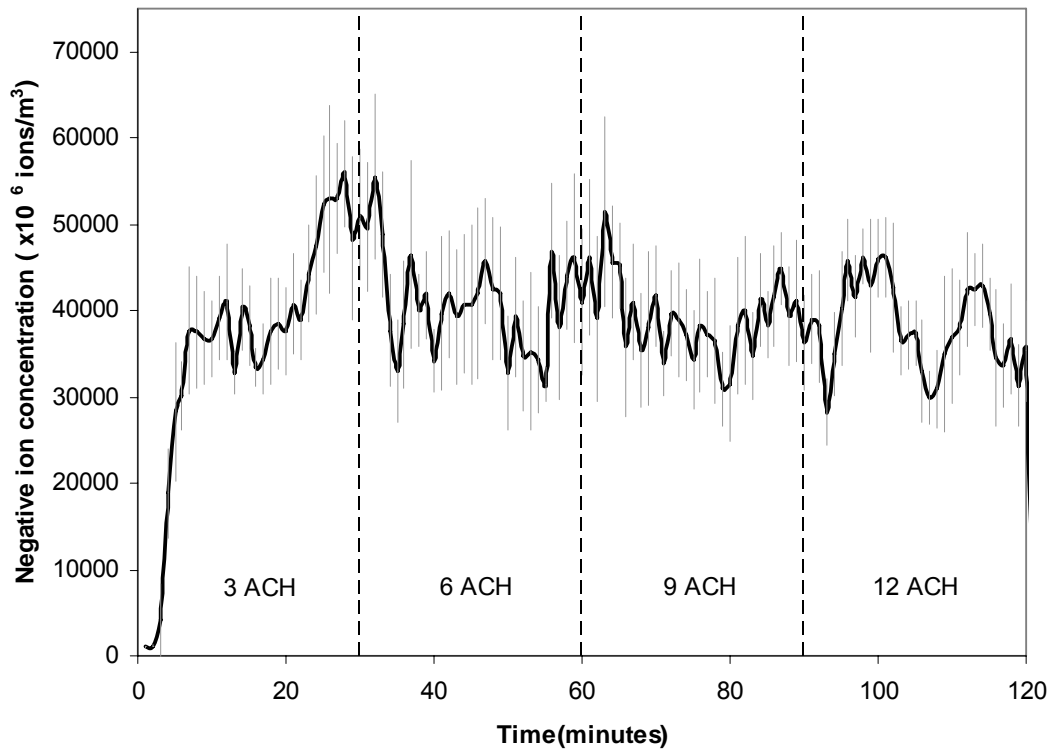


(b) Negative ion concentrations for Sharp plasmacluster device operating in 'negative only' mode

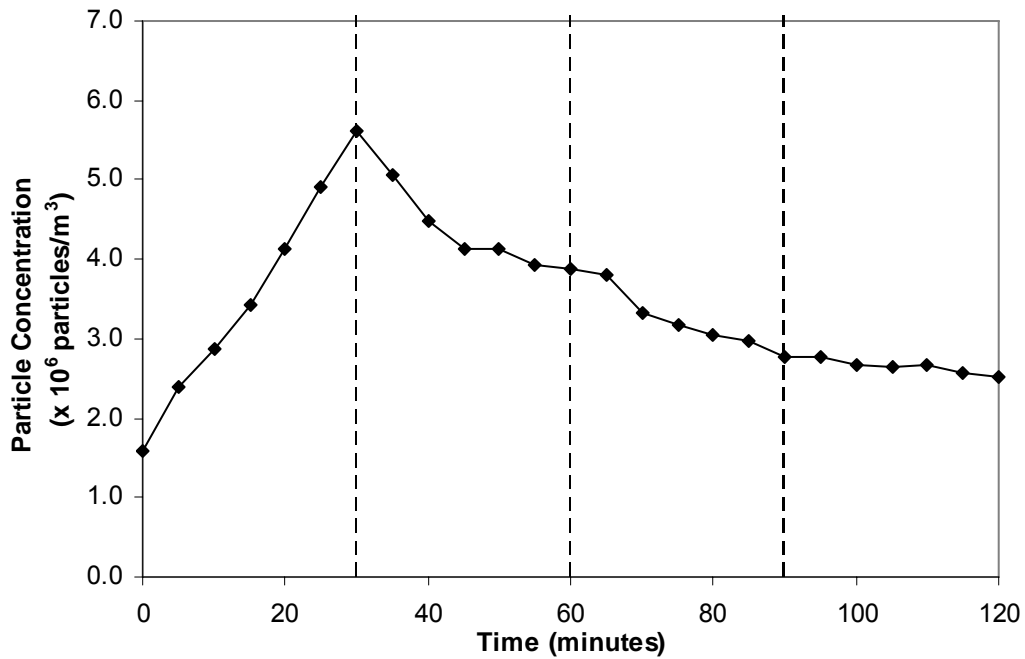


(c) Positive ion concentrations for Sharp plasmacluster device operating in ‘bipolar’ mode

Figure 2: Effect of ventilation rate on mean ion concentration Three experiments shown in each case and error bars represent one standard deviation.



(a) Averaged Ion Concentration. Error Bars indicate one standard deviation of the averaged data.



(b) Particle concentration of  $<0.5 \mu\text{m}$  diameter particles.

Figure 3: Data recorded at ventilation rates of 3, 6, 9 and 12 AC/h for the Aircare negative ioniser.

The lack of influence of the ventilation rate is also apparent in Figure 3(a) where typical measured ion concentrations for the Aircare ioniser generating negative ions are presented. This data is sampled at 0.5 s intervals then averaged over one minute periods, with the error bars representing one standard deviation. From these results it can be seen that the ions do not respond in the same way as aerosol particles in a ventilated room, where an increase in ventilation rate would produce a proportional decrease in particle concentration. However such behaviour can be seen in Figure 3(b) which presents the measured particle concentration for particles  $<0.5\mu\text{m}$  diameter logged at 5 minute intervals during the same experiment.

The results of the decay experiment for the Aircare ioniser are presented in Figure 4, which shows the negative ion decay curves at four ventilation rates. In order to allow comparison of the four cases, the ion concentration is presented as a relative value, with the actual ion concentration,  $n$ , divided by the mean steady state concentration at 3 ACH,  $n_{o3}$ . In all cases when the ioniser is switched off at  $t = 30\text{mins}$ , the ion concentration decays to a steady-state value between  $450 \times 10^6$  and  $700 \times 10^6$  ions/ $m^3$  within approximately 10 minutes. Similar decay rates were also obtained using the Plasmacluster device generating either negative or positive ions.



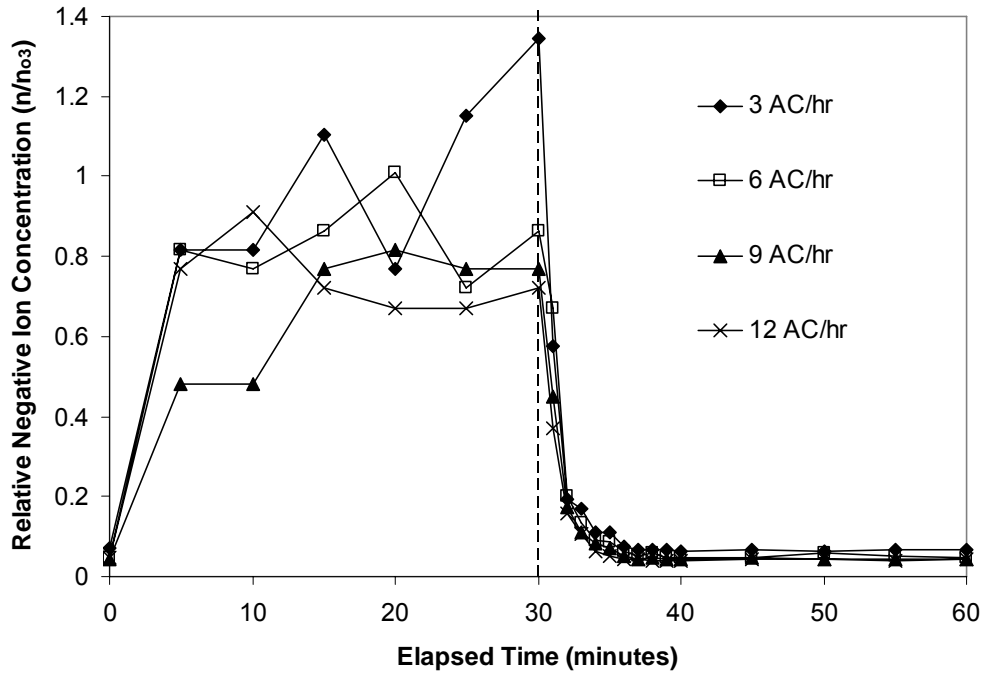


Figure 4: Negative ion concentration decay rate with the Aircare device in operation.

The ion decay curves presented in Figure 4 are wholly consistent with the results of the steady-state experiments. The shape of the decay curve is almost identical for all four cases, again indicating that the ventilation rate has a minimal effect in the ion decay rate in the chamber. Indeed, the actual removal rate of ions from the room is much faster than would be expected through ventilation removal alone assuming uncharged aerosol particles. For example, at 3 AC/h the ventilation system would require about 46 minutes to reduce a particle concentration by 90%. Yet, at 3 AC/h the ion concentration decays by this amount in less than 10 minutes.

#### 4. Theoretical Study

The experimental results suggest that the primary mechanism governing the concentration of ions in the chamber is not the ventilation and that other mechanisms are involved. To better understand the behaviour exhibited in the experiments, and in particular the factors that affect removal of ions from indoor rooms, a theoretical model was developed by extending Mayya et al's [2] work on negative ionisers to include positive ions and sub-micron particles. This was used to and applying this to an ioniser in a ventilated room.

##### 4.1 Model Description

The balance of negative,  $n$ , and positive,  $p$ , ions in a general, fully mixed, space can be described by equations (1) and (2) respectively.

$$\frac{dn}{dt} = q_n - \alpha np - \beta nA \quad (1)$$

$$\frac{dp}{dt} = q_p - \alpha np - \beta pA \quad (2)$$

Here  $q_n$  and  $q_p$  are the generation rate of negative and positive ions,  $\alpha$  represents the recombination rate of ions with those of opposite polarity, and  $\beta$  is the rate of combination of ions with aerosol particles,  $A$ . Typical values for  $\alpha$  and  $\beta$  are given by Horrak [12] as  $\alpha \approx 1.5 \times 10^{-6} \text{ cm}^3/\text{s}$  and  $\beta \approx 1-2 \times 10^{-6} \text{ cm}^3/\text{s}$ . These equations are applicable for general air ions in the atmosphere [6,11,12], however in mechanically ventilated rooms the ion concentrations are also affected by the external ion concentration, the air flow rate through the room and the removal of ions by deposition onto surfaces in the room. As shown by Mayya et al, these effects can be included by modifying equations (1) and (2) to give the rate of change of negative and positive ion concentrations in the room as:

$$\frac{dn}{dt} = q_n - \alpha np - \beta nA + n_o \frac{Q}{V} - n \frac{Q}{V} - \lambda_i n \quad (3)$$

$$\frac{dp}{dt} = q_p - \alpha np - \beta pA + p_o \frac{Q}{V} - p \frac{Q}{V} - \lambda_i p \quad (4)$$

Here  $n_o$  and  $p_o$  are the negative and positive ion concentrations external to the room,  $Q$  ( $\text{m}^3/\text{s}$ ) is the room ventilation flow rate and  $V$  ( $\text{m}^3$ ) is the room volume. The term  $Q/V$  in equations (3) and (4) is equivalent to the air change rate,  $N$ , in this case with units of air changes/second. The rate term  $\lambda_i$  represents the additional removal of ions from the space due to electrical deposition on the walls, and is discussed below.

Aerosol particles in the space can also be modelled by a similar equation [2] to express changes in particle concentration,  $A$ , due to particle generation,  $q_A$ , ventilation rate and rate of electrical deposition,  $\lambda_A$ .

$$\frac{dA}{dt} = q_A - A \frac{Q}{V} - \lambda_A A$$

During the experiments the particle generation rate is small as there is no activity in the chamber and filtration on the ventilation system limits the inflow of external particles greater than  $0.3 \mu\text{m}$  diameter, resulting in measured particle concentrations in the room of the order of  $1 \times 10^7$  particles/ $\text{m}^3$  for  $0.3 \mu\text{m}$  particles down to as low as  $1 \times 10^3$  particles/ $\text{m}^3$  for  $>5\mu\text{m}$  particles. At concentrations of this order of magnitude the removal by electrostatic forces can be neglected [13] and the concentration of particles  $>0.3\mu\text{m}$  diameter in the space,  $A$ , can be approximated by

$$\frac{dA}{dt} = q_A - A \frac{Q}{V} \quad (5)$$

As well as these larger airborne particles, it is likely that sub-micron particles  $< 0.3 \mu\text{m}$  in diameter may be present in room air. The concentration of these particles in the fully mixed room space is also governed by the generation rate, ventilation rate and electrostatic deposition and can be modelled by a fourth concentration variable,  $B$ .

$$\frac{dB}{dt} = q_B - B \frac{Q}{V} - \lambda_B B \quad (6)$$

In the experimental set-up these are likely to be introduced to the room space from outside by the ventilation system as particles of this size will pass through the HEPA filter. Although it was not possible to measure the concentration of these sub-micron particles in the

experiments, they can be approximated in the model through a fourth concentration variable,  $B$ , which is also dependant on the ventilation rate and the generation rate,  $q_B$ , of sub-micron particles. In this case an electrostatic deposition removal term,  $\lambda_B$ , is also included as it is likely that the concentrations of the sub-micron particles may be sufficient for this additional removal mechanism to be significant.

The rate constants  $\lambda_i$  and  $\lambda_B$  can be evaluated by modifying Mayya et al's [2] equations to include positive ions and express the removal rate in terms of the total ionic space charge,  $q_e$ , the ion mobility  $b$ , permittivity of free space ( $\epsilon_0 = 8.854 \times 10^{-12} \text{ C}^2/\text{Nm}^2$ ) and the charge on the sub-micron particles,  $q_c$ . In the case of ions the removal can be given by

$$\lambda_i = \frac{b}{\epsilon_0} (q_e + q_c e B) \quad (7)$$

For small air ions the mobility is typically  $2.4 \times 10^{-6} \text{ m}^2/\text{Vs}$  [12]. The space charge density depends on the relative positive and negative ion concentrations and the elementary charge,  $e = 1.6 \times 10^{-19} \text{ C}$  through the expression

$$q_e = en - ep \quad (8)$$

The enhanced deposition of particles due to the electric field can also be approximated from Mayya's study to give

$$\lambda_p = \frac{D_p}{D_i} q_c \lambda_i \quad (9)$$

where  $D_p$  and  $D_i$  represent the particle and ion diffusion coefficients respectively and have typical values of  $D_p = 1.3 \times 10^{-10} \text{ m}^2/\text{s}$  and  $D_i = 1 \times 10^{-7} \text{ m}^2/\text{s}$  [13].

The parameter  $q_c$  represents the characteristic number of charges acquired by particles due to diffusion charging in the ion field. This is a complex process that depends on the physics of the ion-particle interactions and the duration of the particle in the space. However to get a feel for the relative impact of the ions on particle behaviour an approximation is made based on the charging equations presented by Harrison [6] to give

$$q_c = \frac{4\pi\epsilon_0 d_p kT}{e^2} \left[ \ln \left[ 1 + \frac{d_p c p e^2 t}{4\epsilon_0 kT} \right] - \ln \left[ 1 + \frac{d_p c n e^2 t}{4\epsilon_0 kT} \right] \right] \quad (10)$$

Here  $k$  is the Boltzmann constant ( $= 1.381 \times 10^{-23} \text{ J/K}$ ) and  $T$  is the absolute temperature ( $\sim 300 \text{ K}$ ) and  $c$  is the thermal speed of the ions ( $\sim 300 \text{ m/s}$ ). The particle diameter is given by  $d_p$  and the time,  $t$ , is the average time the particle spends in the room which can be approximated by the reciprocal of the ventilation rate.

Figure 5 uses equation 10 to consider the charging on sub-micron particles of  $0.1$  and  $0.01 \mu\text{m}$  diameter due to negative ions only over a 600s period, equivalent to the mean residence time at  $6 \text{ AC/h}$ . This indicates that at typical ion concentrations achievable with an ioniser in a real room, the number of unit charges acquired by sub-micron particles are likely to be of the order 1 to 10 during their residence in the room. For the purposes of simplifying the model the characteristic number of unit charges carried by these small particles is approximated as  $q_c =$

5. This concurs with Mayya et al's [2] study which showed that as the particle diameter decreased the characteristic charge distribution had a well defined peak, with  $0.1\mu\text{m}$  particles typically carrying around 10 unit charges.

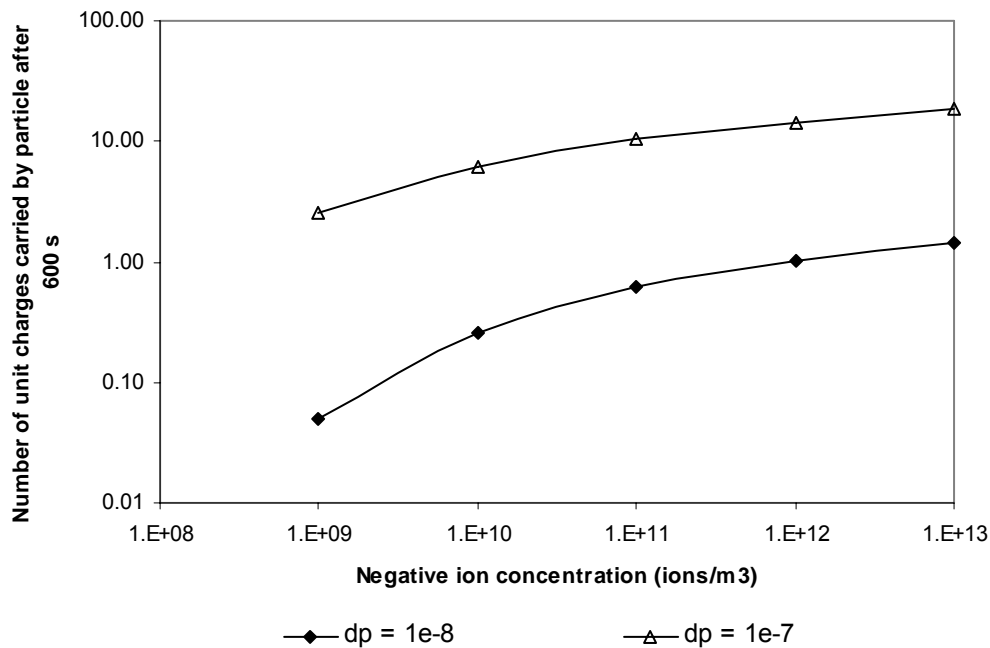


Figure 5: Unit charges acquired by sub-micron particles over a 600s time period.

Equations (3-9) represent a complex non-linear system which cannot be solved analytically. Therefore the model was used to simulate the ion concentrations over time by formulating the equations using a simple differencing scheme with a fixed time-step  $\Delta t$ . A numerical routine was written in VBA using Excel (Microsoft, USA) to solve the equations in 2s time steps.

#### 4.2 Theoretical Model Results

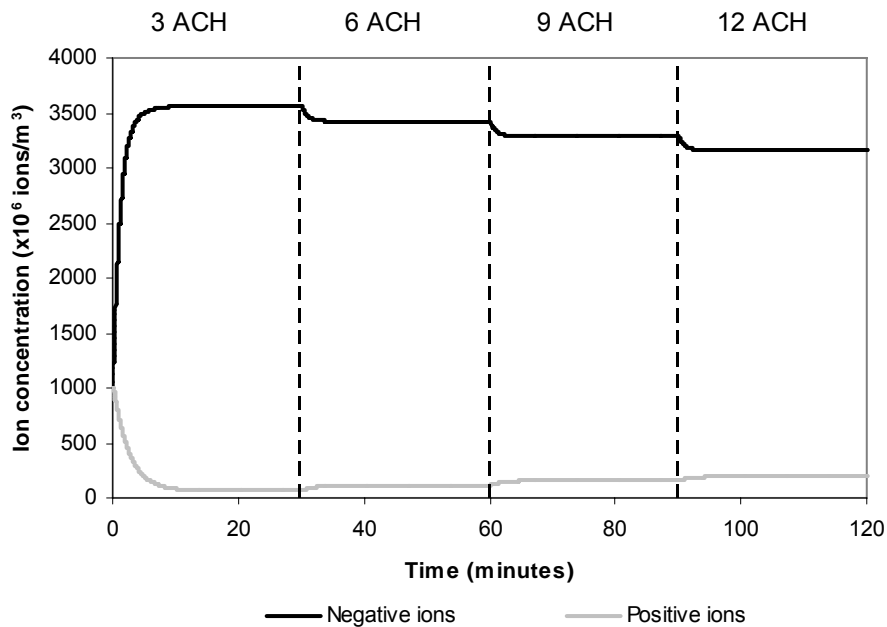
A theoretical ion generation rate was calculated from the mean experimental data at a ventilation rate of 12 AC/h, hence all the subsequent data is relative to the concentration in this case. The model was then used to simulate the steady-state behaviour exhibited by the Aircare negative ioniser in the experimental study. The model was set up to mimic this experiment, with the ventilation rate initially set at 3 AC/h and then increased to 6, 9 and 12 AC/h at 30 minute intervals. The initial conditions, outdoor ion concentrations and ion and particle generation rates are as given in Table 1. These are all theoretical values, chosen to give resulting ion and particle concentrations in the room of a similar order of magnitude to that achieved during the experiments. It should be noted that in the first instance the model is run without the inclusion of sub-micron particles.

Figure 6 shows the resulting simulated ion and particle concentrations for the conditions given in Table 1. It can be seen from these figures that the behaviour of the simulation is similar to that exhibited in the steady-state experiments. The concentration of both positive and negative ions changes very little with increased ventilation rate, while there is a proportional drop in the particle concentration, as expected. The positive ions remain at very low levels throughout the simulation as the only positive ions present are those that enter the chamber from the external air via the ventilation system. Negative ions are generated in the room, and the model predicts that the concentration quickly reaches a steady state at a

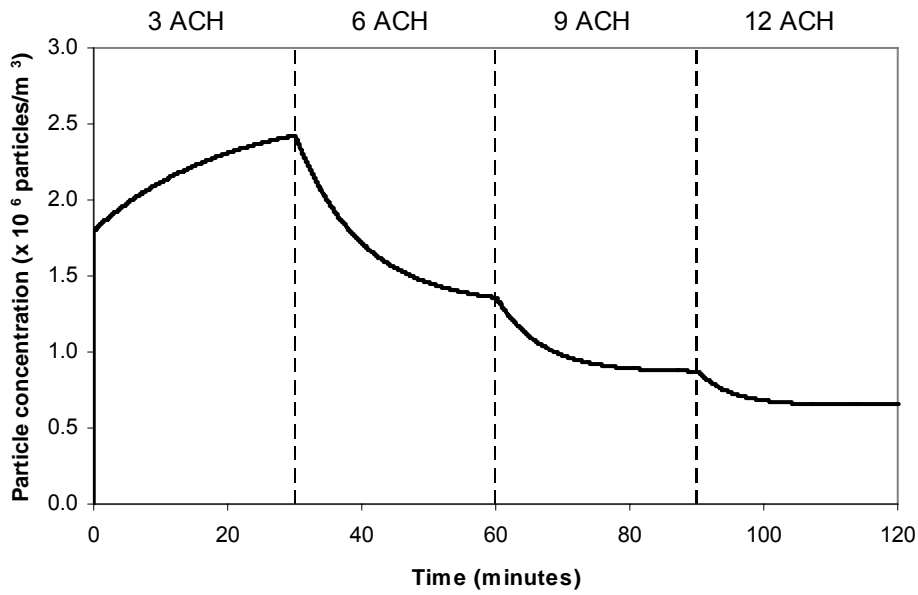
ventilation rate of 3 AC/h and drops by less than 5% at each incremental increase in the ventilation rate.

Table 1: Conditions used in model to simulate the behaviour in the experiments involving negative ion generation

<b>Generation rates</b>	
Negative ions	$3.47 \times 10^7$ ions/m <sup>3</sup> s
Positive ions	0.0 ions/m <sup>3</sup> s
Particles (A)	$2.17 \times 10^3$ particles/m <sup>3</sup> s
Sub-micron particles (B)	0.0 particles/m <sup>3</sup> s
<b>Outdoor ion concentrations</b>	
Negative ions	$5.0 \times 10^8$ ions/m <sup>3</sup>
Positive ions	$5.0 \times 10^8$ ions/m <sup>3</sup>
<b>Initial conditions</b>	
Negative ion concentration	$1.0 \times 10^9$ ions/m <sup>3</sup>
Positive ion concentration	$1.0 \times 10^9$ ions/m <sup>3</sup>
Particle concentration	$1.8 \times 10^6$ particles/m <sup>3</sup>
Sub-micron particle concentration	0.0 particles/m <sup>3</sup>



(a) Concentration of negative and positive ions



(b) Concentration of particles  $>0.3 \mu\text{m}$

Figure 6: Predicted effect of ventilation rate on ion and particle concentration in  $32\text{m}^3$  room, assuming continuous negative ion generation in the space.

Figure 7 shows the predicted ion concentrations from a second simulation where sub-micron particles are included in the model with a generation rate two orders of magnitude greater than the larger particles of  $2.17 \times 10^5$  particles/m<sup>3</sup> s and an initial concentration of  $1.8 \times 10^6$  particles/m<sup>3</sup>. In this case the results are if anything more similar to the experimental data with the predicted curve showing a peak in ion concentration at 3 AC/h and then an almost completely flat profile at the other three ventilation rates that is also apparent in Figure 3. Although the particle concentrations are not shown for this case, the larger particles are as in Figure 6(b) and the sub-micron particles show a similar profile with a peak concentration of approximately  $200 \times 10^6$  particles/m<sup>3</sup>

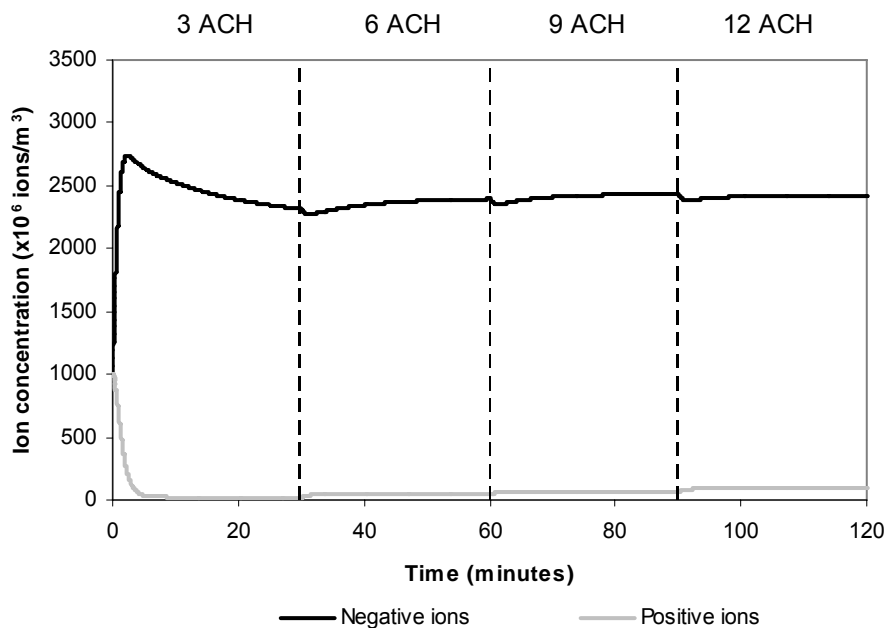


Figure 7: Predicted effect of ventilation rate on ion concentrations including influence of sub-micron particles.

The reason for the difference in the behaviour of particles and ions in the room is explored by considering a decay scenario. Figure 8 shows a simulated ion decay in the chamber when the ion production ceases at  $t = 0$  minutes and the ventilation rate is constant at 6 AC/h. Four different cases are presented; the full model, neglecting the presence of sub-micron particles ( $B = 0$ ), neglecting the electrostatic wall losses ( $\lambda_i = \lambda_B = 0$ ) and removal by ventilation only ( $\alpha = \beta = \lambda_i = \lambda_B = 0$ ). In all cases the outdoor ion concentration is assumed to be zero, the ion generation rate for both positive and negative ions is zero and initial concentrations of positive and negative ions are assumed to be  $5000 \times 10^6$  and  $10000 \times 10^6$  ions/m<sup>3</sup> respectively. The particle generation rate and initial value for the  $>0.3\mu\text{m}$  particles are as given in Table 1 and the generation rate and initial value for the sub-micron particles as for the simulation in Figure 7.

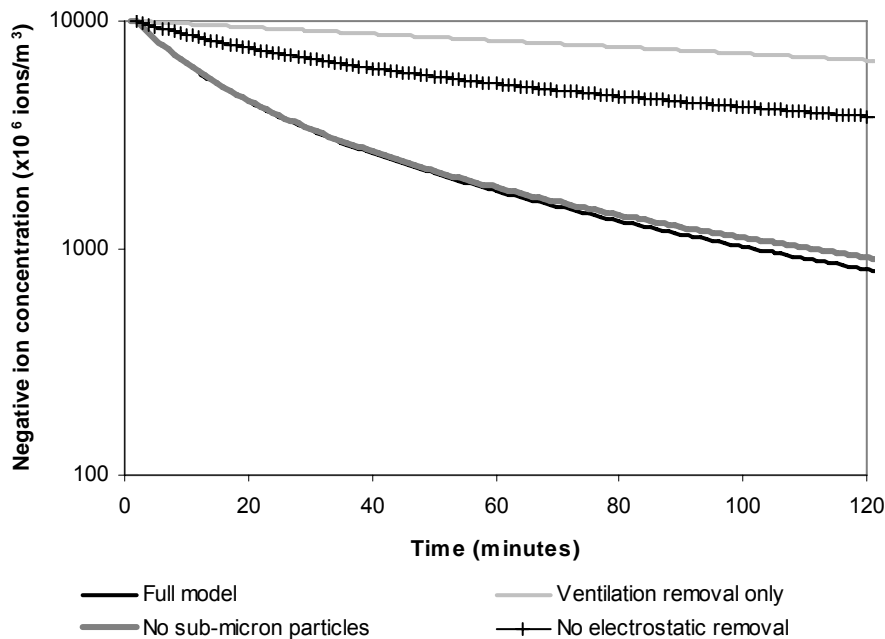


Figure 8: Effect of removal mechanisms on decay rate of ions at 6 ACH.

The simulated ion concentrations in Figure 8 explain why the decay rate of ions measured during the experiments was much greater than expected by ventilation removal alone. The model including only ventilation removal yields the expected first order decay curve however the additional removal mechanisms in the model result in the faster decay rate of ions similar to that seen in the experiments. The results in Figure 8 show that in a typical room with an ioniser in operation the combined removal mechanisms of ion-ion and ion-particle recombination, together with ion loss to the walls, are significant and responsible for a decay rate curve which does not follow a first order approximation. They also demonstrate the dependence of the various decay rates on the negative ion concentration. The ventilation removal rate is a constant value determined by the room ventilation rate, and therefore appears as a straight line in Figure 8. However both the recombination and wall deposition rates are non linear, with the recombination rate a function of the relative positive ion concentration and the wall deposition dependant on both positive and negative ion concentrations. Hence in Figure 8, when the ion concentrations are high, the gradient of the decay curve is much steeper with the additional removal mechanisms than with ventilation removal alone. When the negative (and the positive) ion concentration reduces, the gradient of the curve also reduces, approaching that of the ventilation removal and indicating that the relative influence of wall deposition is less.

The influence of the wall deposition rate can be explored further by considering equations (3), (7) and (8) with  $n_o = 0$  and in the absence of positive ions and particles. This yields a quadratic equation for the negative ion concentration under steady state conditions.

$$\frac{be}{\epsilon_o} n^2 + n \frac{Q}{V} - q_n = 0 \quad (11)$$

Plotting the solution of equation (11) with negative ion generation rate  $q_n$  against the ventilation only removal (Figure 9) reinforces further the impact of the enhanced electrostatic deposition at high ion concentrations. At low ion generation rates, electrostatic deposition at the wall has little influence on air ion concentration, with the latter governed by the ventilation removal. However as the generation rate increases, the wall deposition becomes increasingly dominant, with the result that the rate of increase in the overall ion concentration becomes progressively less and less.

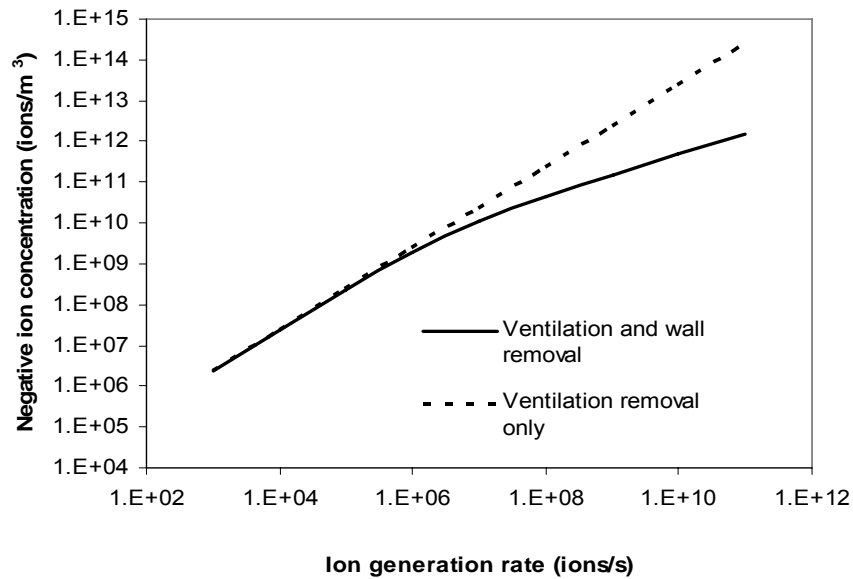


Figure 9: Effect of electrical wall deposition on the concentration of negative ions in the room at a ventilation rate of 1.5 AC/h

## 5. Discussion

The combination of experimental and theoretical results presented above yield some useful insights into the actions of negative air ionisers in indoor air. It is clear from both the experimental evidence and the theoretical results presented in Figures 8 and 9 that the concentration of ions in a room depends on factors that are governed by the rate at which ions are generated within the space. For example, in the absence of an ioniser within the room space, ion generation is typically low and primarily due to infiltration from outdoors. Under such conditions, the concentration of ions in the room will be dominated by the ventilation rate, with additional removal due to ion-ion interactions, while electrically enhanced wall deposition will be minimal; although possibly significant enough to explain why both positive and negative ion counts are lower within buildings than they are outside. However at higher ion generation rates, for example when an ioniser is located in a room, as the results in Figures 8 and 9 suggest, the electrodynamic effects due to the ions become increasingly more important. The ion-ion recombination rate increases with both negative and positive ion concentrations resulting in enhanced ion removal at high concentrations. Wall deposition has a quadratic relationship with the ion concentration, and rapidly becomes the dominant ion



removal mechanism as the ion generation is increased. As seen in both the experimental and theoretical results, the ventilation rate has little impact on the room ion concentration under normal operation of an ioniser, for either positive or negative ions.

Due to technical limitations we were unable to measure the effect of the air ions on aerosol particles with mean diameters less than  $0.3\mu\text{m}$ . Particles of this size are small enough to pass through the HEPA filters serving the chamber and therefore would have entered the room space. In the chamber it is likely these small particles played an important role because they would have been the first aerosol particles to collide with the ions in the air forming highly mobile small cluster ions [8]. Although the theoretical study included the effect of these sub-micron particles, it is difficult to draw firm conclusions about their significance in the absence of experimental data. However, the similarity between the simulated results in Figure 7 and the experimental results in Figures 2 and 3 suggest that the estimated sub-micron particle generation rates used in the theoretical model are of the right order of magnitude and it is therefore possible to draw some general conclusions about the operation of ionisers in indoor air. The ions within the space generate an electric field,  $\underline{E}$ , which exerts a force on particles carrying a charge  $q$  in the space  $\underline{F} = q\underline{E}$ . It is this force that is responsible for the increased removal rate of ions from the room. This force will also act on particles in the space which will acquire a charge through diffusion charging due to ions [6]. Hence as the ion generation rate increases, the electric field strength will increase and the electrophoretic forces on both ions and particles have a greater effect. Although the charging of particles is not considered to any great extent in this study, it is clear from Figure 9 that for an ioniser to result in any significant electrodynamic effects the ion generation rate must be higher than  $\sim 10^8$  ions/s, with an ion concentration in the room space of  $10^{10}$  ions/m<sup>3</sup> or greater. This has implications for the design and application of ionisers as room air cleaning devices. Installation of devices that produce insufficient numbers of ions for the room space are unlikely to be effective as air cleaning devices, however further research quantifying the effect of ionisers on particles is necessary to fully substantiate these values.

## 6. Conclusions

The experimental and theoretical results presented here examine the factors that influence the concentration of ions in ventilated indoor environments. From these it can be concluded that in rooms without any artificial ion generation, the concentration of both positive and negative ions is controlled by the ventilation rate. However with an ioniser operating, the electrical effects become increasingly important as the ion generation rate increases, with the ventilation rate having a negligible effect on the net ion concentration in the space.

## Acknowledgements

The authors would like to express their gratitude to Karen Stevens who assisted with collecting the ion concentration data and to acknowledge the support of EPSRC in funding this study.

## References

1. Kerr KG, Beggs CB, Dean SG, Thornton J, Donnelly JK, Todd NJ, Sleigh PA, Qureshi A, Taylor C: Air ionisation and colonisation/infection with methicillin-resistant *Staphylococcus aureus* and *Acinetobacter* species in an intensive care unit: *Int Care Med* 2006; 32(2): 315-317.
2. Mayya YS, Sapra BK, Khan A., Sunny F: Aerosol removal by unipolar ionization in indoor environments: *J Aerosol Sci* 2004; 35: 923-941

3. Phillips G, Harris GJ, Jones MW: Effects of air ions on bacterial aerosols: *Int J Bacteriol* 1964; 8: 27-37
4. Kellogg EW, Yost MG, Barthakur N, Kreuger AP: Superoxide involvement in the bactericidal effects of negative air ions on *Staphylococcus albus*. *Nature* 1979; 281(5730): 400-401
5. Fletcher LA, Gaunt LF, Beggs CB, Shepherd SJ, Sleigh PA, Noakes CJ, Kerr KG: Bactericidal action of positive and negative ions in air: *BMC Microbiol* 2007; 7: 32
6. Harrison RG: Aerosol charging and radioactivity. PhD thesis, University of London 1992
7. Sakata S, Okada T: Effect of humidity on hydrated cluster-ion formation in a clean room corona discharge neutralizer: *J Aerosol Sci* 1994; 25: 879-893
8. Hawkins LH: Air ions and office health: *Occ Health* 1982; 34(3): 116-124
9. Lee BU, Yermakov M, Grinshpun SA: Removal of fine and ultrafine particles from indoor air environments by unipolar ion emission: *Atmos Environ* 2004; 38: 4815-4823
10. Grabarczyk Z: Effectiveness of indoor air cleaning with corona ionisers: *J Electrostatics* 2001; 51-52: 278-283
11. Hoppel WA: Ion-aerosol attachment coefficients, ion depletion and the charge distribution on aerosols: *J Geophys Res* 1985; 90: 5917-5923
12. Horrak U: Air ion mobility spectrum at a rural area. PhD thesis, University of Tartu, Estonia, 2001
13. Noakes CJ, Sleigh PA, Beggs CB: Modelling the air cleaning performance of negative air ionisers in ventilated rooms. *Roomvent* 2007, Helsinki; 13-15<sup>th</sup> June